RESEARCH ARTICLE | DECEMBER 01 2017

Palmitate Conditions Macrophages for Enhanced Responses toward Inflammatory Stimuli via JNK Activation FREE

Marta Riera-Borrull; ... et. al

Related Content

Tribbles 3: A Novel Regulator of TLR2-Mediated Signaling in Response to *Helicobacter pylori* Lipopolysaccharide

J Immunol (February,2011)

Acylation of cell-associated IL-1 by palmitic acid.

J Immunol (October,1991)

Palmitate-induced MMP-9 expression in the human monocytic cells: Significance in metabolic inflammation

J Immunol (May,2016)

Palmitate Conditions Macrophages for Enhanced Responses toward Inflammatory Stimuli via JNK Activation

Marta Riera-Borrull,*,†,1 Víctor D. Cuevas,*,1 Bárbara Alonso,* Miguel A. Vega,*
Jorge Joven,† Elena Izquierdo,*,2 and Ángel L. Corbí*,2

Obesity is associated with low-grade inflammation and elevated levels of circulating saturated fatty acids, which trigger inflammatory responses by engaging pattern recognition receptors in macrophages. Because tissue homeostasis is maintained through an adequate balance of pro- and anti-inflammatory macrophages, we assessed the transcriptional and functional profile of M-CSF–dependent monocyte-derived human macrophages exposed to concentrations of saturated fatty acids found in obese individuals. We report that palmitate (C16:0, 200 μM) significantly modulates the macrophage gene signature, lowers the expression of transcription factors that positively regulate IL-10 expression (MAFB, AhR), and promotes a proinflammatory state whose acquisition requires JNK activation. Unlike LPS, palmitate exposure does not activate STAT1, and its transcriptional effects can be distinguished from those triggered by LPS, as both agents oppositely regulate the expression of CCL19 and *TRIB3*. Besides, palmitate conditions macrophages for exacerbated proinflammatory responses (lower IL-10 and CCL2, higher TNF-α, IL-6, and IL-1β) toward pathogenic stimuli, a process also mediated by JNK activation. All of these effects of palmitate are fatty acid specific because oleate (C18:1, 200 μM) does not modify the macrophage transcriptional and functional profiles. Therefore, pathologic palmitate concentrations promote the acquisition of a specific polarization state in human macrophages and condition macrophages for enhanced responses toward inflammatory stimuli, with both effects being dependent on JNK activation. Our results provide further insight into the macrophage contribution to obesity-associated inflammation. *The Journal of Immunology*, 2017, 199: 3858–3869.

O besity associates with the development of metabolic diseases and correlates with several types of cancer (1, 2). Inflammation underlies the link between obesity and metabolic diseases. So, an excessive nutrient intake results in the

*Centro de Investigaciones Biológicas, Consejo Superior de Investigaciones Científicas, 28040 Madrid, Spain; and †Unitat de Recerca Biomèdica, Hospital Universitari Sant Joan, Institut d'Investigació Sanitària Pere Virgili, Universitat Rovira i Virgili, 43201 Reus, Spain

accumulation of saturated fatty acids (SFA), which correlates with an increase in proinflammatory cytokines (3). Moreover, adipose and liver tissues from obese individuals are infiltrated by immune cells, primarily macrophages, in what appears to be a primary trigger for obesity-induced inflammation (4, 5). A key role for macrophages in the pathogenesis of metabolic disorders has been demonstrated in mouse models of obesity: defective monocyte recruitment to adipose tissue protects from obesity-induced inflammation (6), and depletion of CD11c+ cells or myeloid cell–specific deletion of IKKβ or JNK1 reduces adipose tissue inflammation (7) and protects mice from insulin resistance (8, 9). Although previous studies have suggested that SFA promote adipose tissue inflammation in a TLR4-dependent manner (10), recent reports suggest that the link between SFA and insulin resistance might not involve a canonical TLR4 activation (11–15).

Inflamed tissues contain macrophages that display a continuum of functional (polarization) states, whose acquisition is dependent on macrophage ontogeny and their surrounding environment (16). Human monocyte-derived macrophages generated in the presence of GM-CSF (GM-MØ) are transcriptionally defined by the expression of a "proinflammatory gene set" and resemble macrophages found in vivo under inflammatory conditions (17–20). Conversely, macrophages generated in the presence of M-CSF (M-MØ) express an "anti-inflammatory gene set" and resemble macrophages from homeostatic/anti-inflammatory settings (17–20). LPS activation of GM-MØ and M-MØ has allowed the identification of novel gene sets whose expression is regulated by LPS in a subtype-specific manner: TLR-mediated activation of GM-MØ results in the production of proinflammatory cytokines (20) and the parallel acquisition of a transcriptional profile that includes a set of genes (referred to as an "activated GM-MØ gene set") whose expression is modified by TLR ligands exclusively in GM-MØ. Regarding M-MØ, their activation leads to release of the

anti-inflammatory cytokine IL-10 (20) and is accompanied by the acquisition of a gene signature that includes genes whose expression is modified by TLR ligands exclusively in M-MØ ("activated M-MØ gene set") (V.D. Cuevas, M.A. Vega, and Á.L. Corbí, unpublished observations).

The molecular mechanisms underlying the activation of human macrophages by SFA have not been completely elucidated. Because mouse macrophage polarization-specific genes cannot be extrapolated to human macrophages (21, 22), we have taken advantage of the above-mentioned human macrophage gene sets to analyze the transcriptional and functional responses of GM-MØ and M-MØ to palmitate. Our results indicate that palmitate triggers a JNK-dependent proinflammatory shift in human macrophages and primes macrophages for exacerbated proinflammatory response toward other pathogenic stimuli. The identification of the genes whose expression correlates with SFA-induced macrophage activation might provide useful biomarkers for the determination of the polarization state of adipose tissue macrophages under homeostatic and pathological conditions.

Materials and Methods

Generation of human monocyte-derived macrophages

Human PBMCs were isolated from buffy coats from normal donors over a Lymphoprep (Nycomed Pharma, Oslo, Norway) gradient according to standard procedures. Monocytes were purified from PBMCs by magnetic cell sorting using anti-CD14 microbeads (Miltenyi Biotec, Bergisch Gladbach, Germany) (>95% CD14$^+$ cells). Monocytes (0.5×10^6 cells/ml, >95% CD14$^+$ cells) were cultured in RPMI 1640 supplemented with 10% FBS for 7 d in the presence of 1000 U/ml GM-CSF or 10 ng/ml M-CSF (ImmunoTools, Friesoythe, Germany) to generate GM-CSF–polarized macrophages (hereafter termed GM-MØ) or M-CSF–polarized macrophages (hereafter termed M-MØ), respectively (23). Cytokines were added every 2 d. Where indicated, macrophages were treated with 10 ng/ml Escherichia coli 055:B5 LPS (Sigma-Aldrich, St. Louis, MO), palmitate (C16:0, 200 μM), or BSA for the indicated periods of time. Cells were cultured in 21% O_2 and 5% CO_2. For intracellular signaling inhibition, macrophages were exposed to JNK inhibitor SP600125 (30 μM) during 1 h before treatment with BSA or palmitate (C16:0).

Fatty acid preparation

Sodium palmitate (P9767; Sigma-Aldrich) and sodium oleate (O7501; Sigma-Aldrich) were prepared by diluting a 200 mM stock solution in 70% ethanol into 10% fatty acid–free, low-endotoxin BSA (A-8806; Sigma-Aldrich; adjusted to pH 7.4) to obtain a 5 mM palmitate-BSA stock solution that was filtered using a 0.22-μm low-protein binding filter (Millipore, Billerica, MA). Palmitate and oleate were added at 200 μM, and BSA/ethanol was used in control treatments. Sodium arachidonate (SML1395; Sigma-Aldrich) was also prepared in BSA and tested at 30 and 100 μM.

Fatty acid uptake

Macrophage fatty acid uptake was evaluated using an Oil Red O staining protocol (24). Briefly, macrophages were fixed with 10% phosphate-buffered formalin for 10 min, rinsed with PBS once, and then rinsed with 60% isopropanol; after that, macrophages were stained with Oil Red O (Sigma-Aldrich) at 37°C for 1 min in darkness. Finally, macrophages were destained with 60% isopropanol, washed with PBS three times, and samples were counterstained with hematoxylin for 5 min before examination by light microscopy.

Quantitative real-time RT-PCR

Total RNA was extracted using the NucleoSpin RNA/protein kit (Macherey-Nagel, Düren, Germany), retrotranscribed, and amplified using the Universal Human Probe library (Roche Diagnostics, Mannheim, Germany). Oligonucleotides for selected genes were designed according to the Roche software for quantitative real-time PCR (Roche Diagnostics). Assays were made in triplicate and results normalized according to the expression levels of TATA box–binding protein (TBP) mRNA. Results were expressed using the ΔΔCT method for quantification. Analyzed genes included the proinflammatory gene set and the anti-inflammatory gene set that have been previously defined (18, 25). Where indicated, microfluidic gene cards were

custom-made (Roche Diagnostics) and designed to analyze the expression of a set of genes whose expression is variably modulated by LPS (10 ng/ml E. coli 055:B5, 4 h) in GM-MØ and/or M-MØ (26) (V.D. Cuevas et al., unpublished observations). Specifically, the gene cards included 10 genes upregulated by LPS in both GM-MØ and M-MØ, 9 genes upregulated by LPS exclusively in GM-MØ, 3 genes downregulated by LPS exclusively in GM-MØ, 28 genes upregulated by LPS exclusively in M-MØ, 20 genes downregulated by LPS exclusively in M-MØ, 78 genes upregulated by LPS in GM-MØ but downregulated in M-MØ, and 9 genes downregulated by LPS in GM-MØ but upregulated in M-MØ. Assays were made in triplicate on two independent samples of each type, and the results were normalized according to the mean of the expression level of endogenous reference genes HPRT1, TBP, and RPLP0. In all cases (quantitative real-time PCR or gene cards), the results were expressed using the ΔΔCT method for quantitation. Nonsupervised hierarchical clustering was done on the scaled expression level of each gene in BSA- and palmitate-treated LPS-activated M-MØ, and using the gplots R package (https://CRAN.R-project.org/package=gplots).

ELISA

Macrophage supernatants were assayed for the presence of cytokines using commercial ELISA kits for TNF-α, CCL2 (BD Biosciences, San Jose, CA), IL-10, IL-6, IL-1β (BioLegend, San Diego, CA), and CCL19 (Sigma-Aldrich) according to the protocols supplied by the manufacturers.

Western blot

Cell lysates were obtained in 10 mM Tris-HCl (pH 8), 150 mM NaCl, 1% Nonidet P-40 lysis buffer containing 2 mM Pefabloc, 2 mg/ml aprotinin/antipain/leupeptin/pepstatin, 10 mM NaF, and 1 mM Na_3VO_4. Ten to fifteen micrograms of cell lysate was subjected to SDS-PAGE and transferred onto an Immobilon polyvinylidene difluoride membrane (Millipore). Protein detection was carried out using Abs against MAFB (sc-10022; Santa Cruz Biotechnology, Santa Cruz, CA), AhR (sc-8087; Santa Cruz), and C/EBPβ (sc-150; Santa Cruz Biotechnology), phospho-ERK1/2, phospho-JNK, phospho-p38, phospho-p65, phospho-IKK, total IKK, ERK1/2, and IKBα (all from Cell Signaling Technology), total and phosphorylated STAT1 and STAT 3 (BD Biosciences), phospho–IFN regulatory factor (IRF)3 (Cell Signaling Technology), and total IRF3 (Santa Cruz Biotechnology). Protein loading was normalized using a mAb against GAPDH (Santa Cruz Biotechnology) or an Ab against human vinculin (Sigma-Aldrich).

Phosphoarrays

Intracellular signaling in response to palmitate was assessed with lysates from macrophages exposed to palmitate for 4 h and using the Proteome Profiler array human phospho-kinase array kit (no. ARY003B; R&D Systems), which detects the relative phosphorylation levels of 46 intracellular serine/threonine/tyrosine kinases, and following the manufacturer's recommendations.

Statistical analysis

Statistical analysis was performed using a Student t test, and $p < 0.05$ was considered significant (*$p < 0.05$, **$p < 0.01$, ***$p < 0.001$).

Results

Palmitate modifies the functional, transcriptomic, and protein profile of human anti-inflammatory M-MØ

Much evidence indicates that macrophage dysfunction in states of lipid excess contributes to the development of obesity-related diseases (6–9). To determine to what extent fatty acid exposure modifies the polarization state of human macrophages, GM-MØ and M-MØ were exposed for 24 h to 200 μM palmitate, a concentration that resembles that found in obese individuals (27–30). Palmitate was efficiently captured by both macrophage subtypes (Supplemental Fig. 1A) and significantly increased the production of TNF-α and IL-1β, diminished the basal levels of CCL2, whose expression is linked to anti-inflammatory polarization (31), and had no effect on IL-10 production by M-MØ (Fig. 1A). At the transcriptional level (Fig. 1B), palmitate drastically downregulated expression of the M-MØ-specific anti-inflammatory gene set (18, 25) (Fig. 1C), whereas it increased the mRNA expression of genes

within the GM-MØ–associated proinflammatory gene set (Fig. 1C). Kinetics analysis revealed that the expression of prototypical genes of the anti-inflammatory gene set (*CCL2*, *IL10*, *HTR2B*, *HTR7*) decreased only 4 h after palmitate treatment, whereas upregulation of genes of the proinflammatory gene set (*INHBA*, *EGLN3*, *TNF*, *IL6*) was seen at later time points after palmitate exposure (Fig. 1D). In the case of GM-MØ, palmitate significantly enhanced the basal production of TNF-α, IL-6, and IL-1β (Fig. 1A), enhanced the mRNA levels of *TNF*, *IL1B*, *IL6*, and *IDO1*, and reduced the expression of various GM-MØ– and M-MØ– specific genes (Supplemental Fig. 1B). The ability of palmitate to downregulate the expression of the M-MØ–specific anti-inflammatory gene set prompted us to determine its effects on the expression of transcription factors that control macrophage polarization (AhR, MAFB, C/EBPβ) (18, 25, 26, 32, 33). M-MØ exhibited higher levels of MAFB and AhR than GM-MØ, whereas the latter exhibit a higher content of C/EBPβ (Fig. 1E). Palmitate treatment significantly reduced MAFB and AhR protein levels, and increased C/EBPβ, in M-MØ (Fig. 1E), changes that were evident 4–10 h after palmitate treatment (Fig. 1F). Therefore, palmitate stimulates M-MØ to reduce the expression of their specific anti-inflammatory gene set and to gain cytokine and transcription factor profiles that resemble GM-MØ. The palmitate-induced downregulation of MAFB protein expression is especially significant given the involvement of MAFB in the acquisition of an anti-inflammatory profile by human macrophages (26).

Palmitate and LPS induce distinct transcriptional profiles in human macrophages

Innate immune cells sense palmitate as a danger signal via the LPS receptor TLR4 (34, 35) as well as additional receptors (34, 36–38). Numerous studies have already defined the LPS-induced transcriptional changes in mouse and human macrophages (39), and we have previously identified LPS-responsive genes in GM-MØ and M-MØ (Fig. 1B) (V.D. Cuevas et al., unpublished observations). Thus, we compared the transcriptional changes elicited on M-MØ by palmitate (200 μM) and LPS (10 ng/ml) exposure for 4 and 24 h. LPS and palmitate differentially modified the expression of the proinflammatory gene set and anti-inflammatory gene set in M-MØ (Supplemental Fig. 2A, 2B), including opposite actions on the expression of *MMP12*, *PPARG1*, *CCR2B*, *IL10*, and *CCL2* after 24 h (Fig. 2A). Moreover, distinct transcriptional responses of M-MØ to LPS and palmitate were also observed upon analysis of a large set of LPS-regulated genes (Supplemental Fig. 2C, 2D), as *IDO1*, *CXCL10*, *MAOA*, *TNFRSF1B*, *EMR2*, *CCL19*, *LAMB3*, and *TRIB3* expression was oppositely modified upon exposure to LPS or palmitate for 4 and 24 h (Fig. 2B, 2C). The presence of IFN-regulated genes (*IDO1*, *CXCL10*) within the list of genes differentially regulated by LPS and palmitate is in agreement with their distinct effect on STAT1, which is only activated in response to LPS (Fig. 2D). Altogether, this set of experiments indicates that palmitate induces a unique and specific transcriptional response in human macrophages, and that the palmitate-induced macrophage proinflammatory shift is only partly reminiscent of that triggered by LPS.

JNK activation mediates the transcriptional changes triggered by palmitate on human macrophages

To search for the basis of the palmitate-specific changes in human macrophages, we screened the phosphorylation state of intracellular signaling molecules after palmitate treatment. Comparison of control and palmitate-treated macrophages showed changes in the phosphorylation state of HSP27, ERK1/2, p27, RSK 1/2/3, c-JUN, and eNOS and identified JNK as the kinase with the higher level of

palmitate-induced activation (Fig. 3A, 3B). Correspondingly, c-Jun was also found to be phosphorylated in M-MØ exposed to palmitate for 4 h (Fig. 3A). The contribution of the palmitate-induced JNK activation to the transcriptional changes promoted by the fatty acid was next assessed using the selective JNK inhibitor SP600125 (Fig. 3C). JNK inhibition significantly impaired the palmitate effect on the expression of *INHBA*, *TNF*, *IL10*, *IGF1*, *MAFB*, and *TRIB3* (Fig. 3D). Additionally, the JNK inhibitor also diminished the palmitate-induced downregulation of MAFB protein expression (Fig. 3E). Therefore, JNK activation mediates the palmitate-dependent modification of the transcriptional profile of human macrophages and contributes to the palmitate-induced loss of MAFB, whose expression is required for the acquisition of the macrophage anti-inflammatory profile (26).

Palmitate conditions the LPS-induced cytokine profile of M-MØ

Macrophages are extremely sensitive to the surrounding extracellular milieu, and their exposure to an initial stimulus determines their subsequent functional responses to additional stimuli (40–43). Because palmitate levels are enhanced in obesity-related pathologies, whose comorbidities include altered inflammatory responses, we hypothesized that palmitate exposure might also condition human macrophages for altered responses to additional stimuli. Thus, we initially assessed whether palmitate influences LPS-initiated intracellular signaling in M-MØ. Palmitate alone caused only a very low NF-κB activation (as illustrated by a weak phosphorylation of p65) (Fig. 4A) and a weak reduction in basal STAT3 phosphorylation levels (Fig. 4B). However, palmitate had a remarkable effect on the intracellular signaling pathways activated by LPS. Specifically, palmitate pretreatment (24 h) led to more potent LPS-induced activation of NF-κB (as evidenced by increased phosphorylation of IKKαβ and p65 and a more profound loss of IkBα, Fig. 4A), lower LPS-induced STAT1 and STAT3 phosphorylation, and higher LPS-induced activation of IRF3, p38 MAPK, and JNK (Fig. 4). Therefore, exposure to palmitate conditions macrophages for altered intracellular signaling in response to another pathogenic stimulus.

Next, we evaluated whether palmitate also modulates the transcriptional responses initiated by LPS in M-MØ. To that end, macrophages were exposed to palmitate (24 h) before stimulation with LPS (4 h), and the expression of the activated M-MØ gene set (Fig. 1B), whose LPS responsiveness is exclusive of M-MØ (V.D. Cuevas et al., unpublished observations), was determined. Palmitate pretreatment greatly altered the LPS-induced transcriptional response, with a profound effect on the expression of the genes upregulated by LPS within the activated M-MØ gene set (Fig. 5A, Supplemental Fig. 3). Specifically, palmitate significantly impaired the LPS-induced upregulation of 25% of the genes whose expression is enhanced by LPS only in M-MØ (Fig. 5B, Supplemental Fig. 3), an effect that was most pronounced on genes with the highest M-MØ–specific upregulation by LPS (*CCL19*, *ARNT2*, *RGS16*, *ADIRF*, *MAOA*) (Supplemental Fig. 3). Regarding the expression of the genes downregulated by LPS within the activated M-MØ gene set (Supplemental Fig. 3), palmitate impaired the LPS-induced downregulation of 20% of them (5 out of 26) and concomitantly potentiated the LPS-induced downregulation of six genes (Fig. 5B, Supplemental Fig. 3). Therefore, exposure to palmitate significantly affects the LPS-regulated gene expression in human macrophages.

Finally, we evaluated whether pre-exposure to palmitate affected the production of LPS-induced cytokines of human macrophages. To that end, M-MØ were exposed to palmitate for 24 h and then stimulated with LPS (Fig. 6A). Palmitate pretreatment significantly
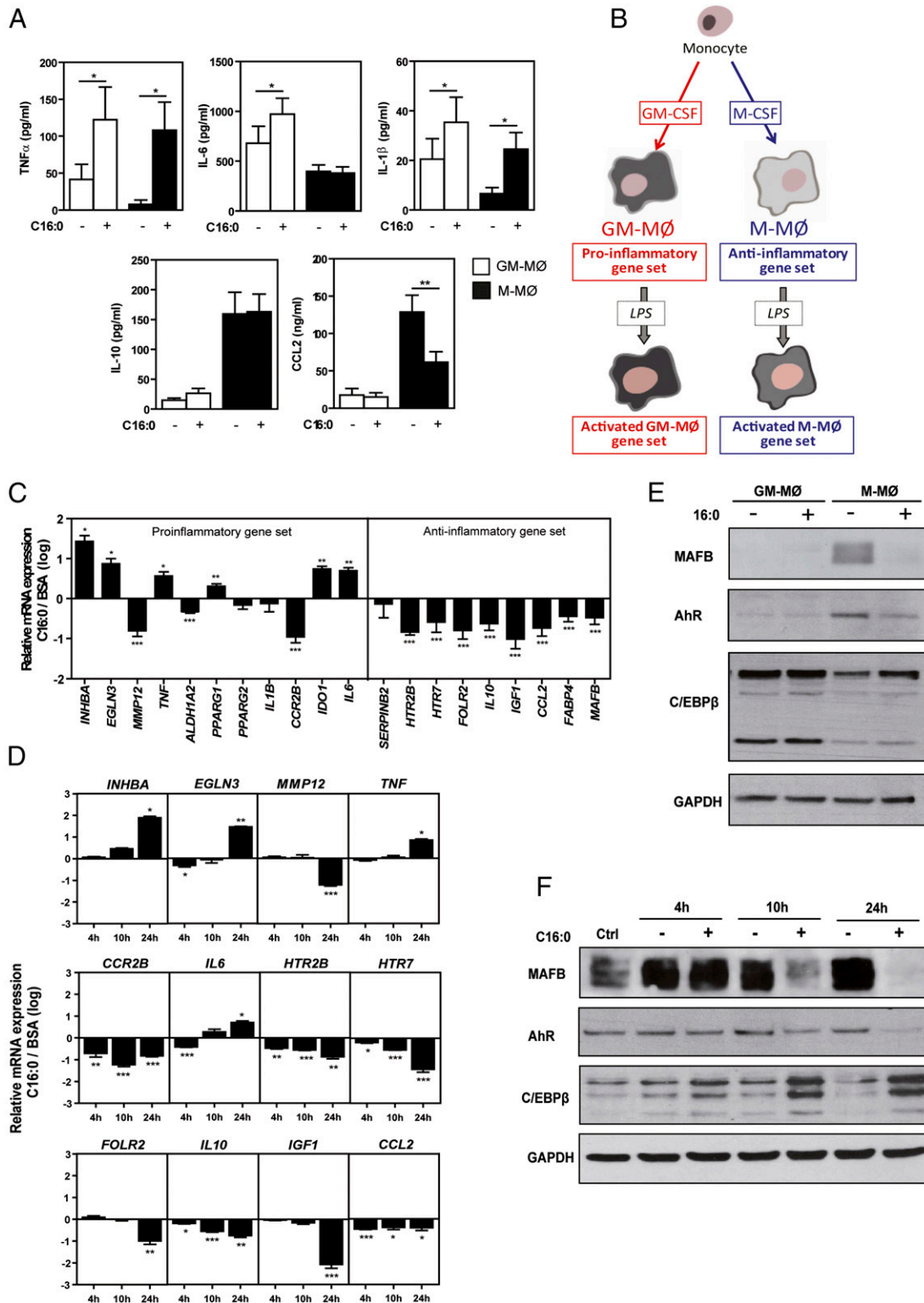
FIGURE 1. Functional, transcriptomic, and transcription factor profile of palmitate-treated human macrophages. (**A**) Levels of the indicated cytokines in the culture media of macrophages (GM-MØ and M-MØ) exposed to 200 μM palmitate (C16:0) or BSA for 24 h, as determined by ELISA. Shown is the mean ± SEM of 10 independent experiments. (**B**) Schematic representation of the relationships between the macrophages transcriptional signatures and defining gene sets used throughout this study. The proinflammatory gene set and anti-inflammatory gene set have been reported in González-Domínguez et al. (25). The activated GM-MØ gene set and activated M-MØ gene set have been derived from the transcriptional analysis deposited in the Gene Expression Omnibus (https://www.ncbi.nlm.nih.gov/geo/query/acc.cgi?acc=GSE99056) under accession number GSE99056 (V.D. Cuevas et al., unpublished observations). (**C**) Relative mRNA expression of the indicated genes in M-MØ exposed to 200 μM palmitate (C16:0) or BSA for 24 h, as determined by quantitative RT-PCR using *TBP* as a reference. The expression of each gene after palmitate treatment and relative to its expression after BSA treatment is indicated. Shown is the mean ± SEM of 10 independent experiments. (**D**) Relative mRNA expression of the indicated genes in M-MØ exposed to 200 μM palmitate (C16:0) or BSA for 4, 10, or 24 h, as determined by quantitative RT-PCR using *TBP* as a reference. The expression of each gene after palmitate treatment and relative to its expression after BSA treatment is indicated. Shown is the mean ± SEM of three independent experiments. (**E**) Expression of MAFB, AhR, and C/EBPβ in macrophages (GM-MØ and M-MØ) treated with 200 μM palmitate (C16:0) or BSA (−) for 24 h, as determined by Western blot. (*Figure legend continues*)

enhanced the LPS induction of the proinflammatory cytokines TNF-α, IL-6, and IL-1β, whereas it inhibited LPS-induced IL-10 and CCL2 production by M-MØ (Fig. 6B). Besides, palmitate pretreatment completely blocked the LPS-induced production of the CCL19 chemokine by M-MØ (Fig. 6B). Therefore, palmitate not only modifies the phenotype and function of anti-inflammatory (M-CSF–dependent) M-MØ but primes M-MØ for increased production of proinflammatory cytokines (and reduced production of anti-inflammatory cytokines) in response to a pathogenic stimulus such as LPS. Importantly, these effects of palmitate are fatty acid specific because the unsaturated free fatty acid oleate (C18:1) was efficiently taken up by human macrophages (Supplemental Fig. 4A), but it neither modified the basal level of expression of MAFB, AhR, and C/EBPβ in M-MØ (Supplemental Fig. 4B) nor altered the LPS-induced production of TNF-α, IL-6, CCL2, and IL-10 (Supplemental Fig. 4C). Similarly, arachidonate (C20:4) did not modify the expression of MAFB and AhR (Supplemental Fig. 4D) and did not impair the LPS-induced production of IL-10 in M-MØ (Supplemental Fig. 4E).

JNK activation mediates the ability of palmitate to condition macrophage responses to LPS

The ability of palmitate to modify the LPS-induced cytokine profile of M-MØ correlates with its capacity to modulate LPS-initiated intracellular signaling (shown in Fig. 4). Such a correlation is especially relevant in the case of JNK, which plays a central role in the development of inflammation in adipose tissue and insulin resistance in animal models (44). Given the ability of palmitate to activate JNK, we analyzed whether the palmitate-induced JNK activation contributes to its macrophage-conditioning effect. Inhibition of JNK activation by SP600125 reduced the palmitate-dependent inhibition in the production of LPS-induced IL-10 (Fig. 6D) although it had no significant effect on the levels of LPS-induced CCL2 (Fig. 6D). Therefore, the palmitate-induced JNK activation modifies the macrophage transcriptome and mediates the ability of palmitate to alter macrophage responses toward pathogenic stimuli such as LPS.

Discussion

Macrophages are critically involved in the initiation and resolution of inflammatory processes, and their deregulated activation contributes to chronic inflammatory diseases (4). In the case of chronic inflammation associated to metabolic syndromes, the production of proinflammatory cytokines by macrophages correlates with the serum concentration of SFA (45), whose increased levels modify macrophage effector functions either by itself (e.g., palmitate) (10) or in combination with high levels of glucose and insulin (46). Taking advantage of the previous identification of gene sets that specifically define the proinflammatory and anti-inflammatory state of human macrophage (18, 25), we now report that palmitate promotes the acquisition of a proinflammatory state that depends on JNK and differs from the LPS-induced proinflammatory activation at the transcriptional and functional levels. Further supporting the specificity of the palmitate-induced macrophage activation, we also provide evidences that palmitate conditions, or trains, human macrophages for stronger proinflammatory responses toward pathogenic stimuli.

Because metabolic diseases are driven by a low-grade inflammation and elevated levels of proinflammatory cytokines (47), the ability of palmitate to condition macrophage responses to other inflammatory stimuli (e.g., LPS) has very relevant pathological implications. It is now well established that metabolic endotoxemia initiates obesity and insulin resistance and, in fact, lowering plasma LPS concentration has been proposed as a strategy to tackle metabolic diseases (48). Consequently, the palmitate proinflammatory conditioning that we now report might exacerbate the proinflammatory responses of monocytes/macrophages toward pathogen-associated molecular patterns (49) (e.g., LPS) derived from bacteria translocating from the gut, thus enhancing the production of pathogen-associated molecular pattern (PAMP)–induced inflammatory cytokines. In agreement with the palmitate-induced increased LPS responsiveness, palmitate conditions macrophages for stronger LPS-induced NF-κB, IRF3, p38, ERK, and JNK signaling. Because NF-κB and JNK are chronically activated in adipose tissue from obese and insulin resistance subjects (50) and JNK activation in mouse macrophages is required for obesity-induced insulin resistance and inflammation (44), the macrophage-conditioning ability of palmitate that we now report might contribute to the known association between bacterial DNA translocation and increased insulin resistance (51).

The macrophage-conditioning ability of palmitate also resembles the effect of PAMPs such as β-glucan, which render macrophages more responsive to a subsequent stimulation by LPS (42, 43). This boosting effect has led to the concept of trained immunity and allowed the demonstration that innate immunity cells such as macrophages produce much higher levels of proinflammatory cytokines when previously exposed to certain training stimuli (42, 43). From this point of view, the changes that we have detected in palmitate-treated macrophages (loss of AhR and MAFB expression, reduced expression of the anti-inflammatory gene set) are compatible with the acquisition of a palmitate-trained state that would confer palmitate-conditioned macrophages with the ability to produce higher levels of proinflammatory cytokines upon exposure to a second stimulus.

The capacity of palmitate to downregulate MAFB protein expression in macrophages is especially relevant for the whole set of transcriptional and functional changes triggered by this SFA. Palmitate exerts rapid transcriptional effects and upregulates the expression of the macrophage proinflammatory gene set (*INHBA*, *EGLN3*) (18, 25) in <24 h, a time at which palmitate has also provoked the loss of the transcription factors that drive anti-inflammatory gene set expression (AhR, MAFB) (18, 25). The loss of MAFB expression appears to critically underlie the proinflammatory ability of palmitate because MAFB is a major positive regulator for the expression of a significant number of genes that characterize anti-inflammatory IL-10–producing macrophages (e.g., *IL10*, *IGF1*, *CCL2*) (26). Importantly, the palmitate-induced loss of MAFB expression is partly mediated by JNK, an effect that is in line with the ability of JNK to promote MAFB ubiquitination (52) and agrees with the known proinflammatory nature of JNK in vivo (44). Besides, MAFB protein levels are also controlled by other kinases such as GSK3β (53), whose activation state might be also affected by palmitate (54). In this regard, note that the diminished LPS-induced production of IL-10 seen in palmitate-treated macrophages can be prevented by lithium chloride, a well-known but nonspecific GSK3β inhibitor (55) (data not shown).

(**F**) Expression of MAFB, AhR, and C/EBPβ in M-MØ nontreated (Ctrl) or treated with 200 μM palmitate or BSA (−) for 4, 10, or 24 h, as determined by Western blot. In (E) and (F), three independent experiments were done and one of them is shown, and GAPDH protein levels were determined in parallel as a protein loading control. *$p < 0.05$, **$p < 0.01$, ***$p < 0.001$.
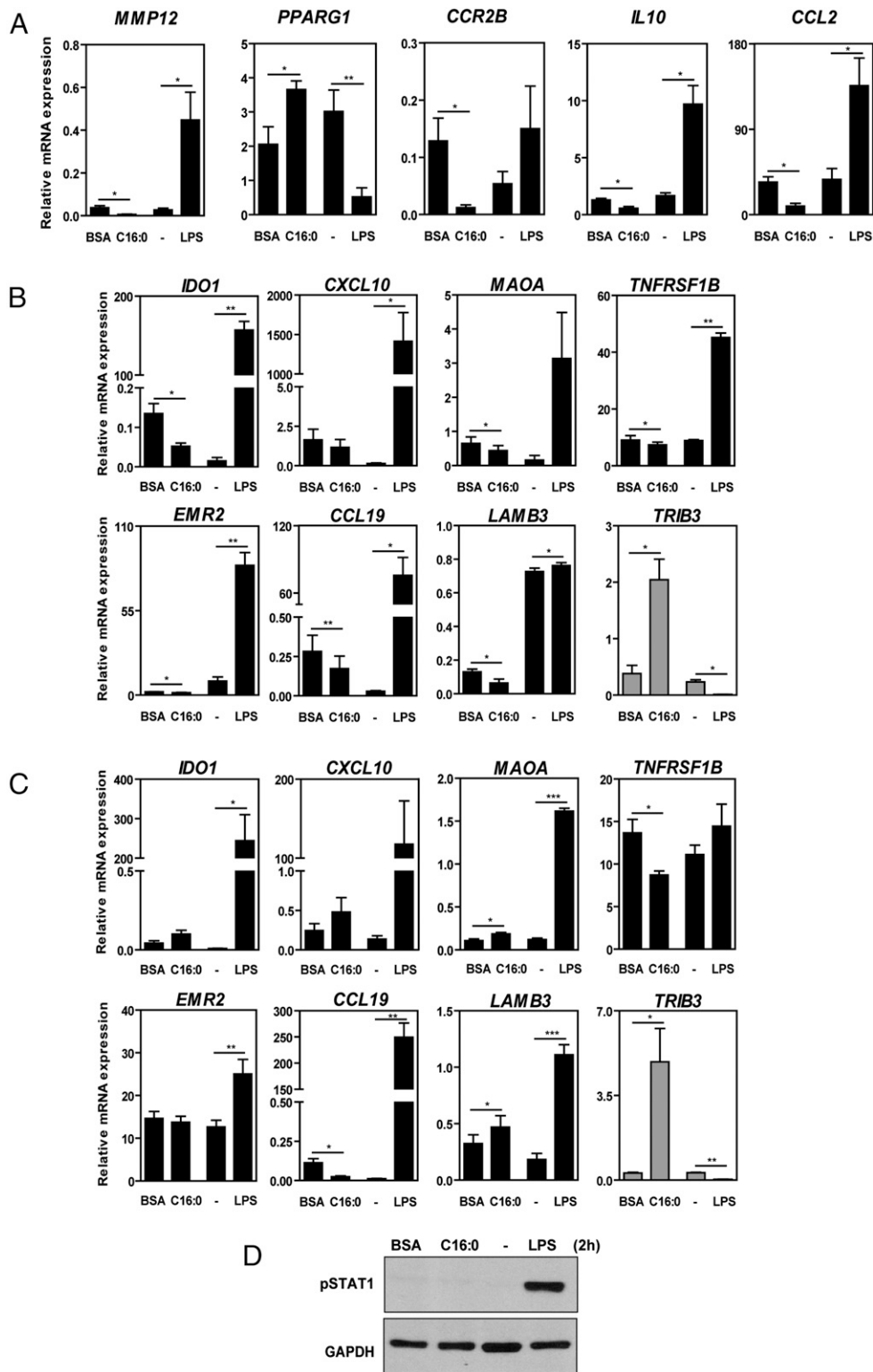
FIGURE 2. Comparison of the transcriptomic changes elicited by palmitate or LPS on human macrophages. (**A**) Relative mRNA expression of the indicated polarization-specific genes in M-MØ untreated (−) or exposed to 10 ng/ml LPS, 200 μM palmitate (C16:0), or BSA for 24 h, as determined by quantitative RT-PCR using *TBP* as a reference. (**B** and **C**) Relative mRNA expression of the indicated LPS-regulated genes in M-MØ untreated (−) or exposed to 10 ng/ml LPS, 200 μM palmitate, or BSA for (B) 4 or (C) 24 h, as determined by quantitative RT-PCR using *TBP* as a reference. In (A)–(C), results are shown as mean ± SEM of five independent experiments. (**D**) Expression of activated STAT1 in M-MØ nontreated (−) or treated with 10 ng/ml LPS, 200 μM palmitate, or BSA for 2 h, as determined by Western blot. GAPDH protein levels were determined in parallel as a protein loading control. *$p < 0.05$, **$p < 0.01$, ***$p < 0.001$.

Previous studies have assumed that palmitate activation of macrophages mostly resembles LPS-induced mechanisms because palmitate is recognized by TLR4 and activates proinflammatory

signaling pathways in vitro and in vivo (10). However, and in line with previous reports (11–13), our results indicate that palmitate and LPS differ in their respective transcriptional and functional
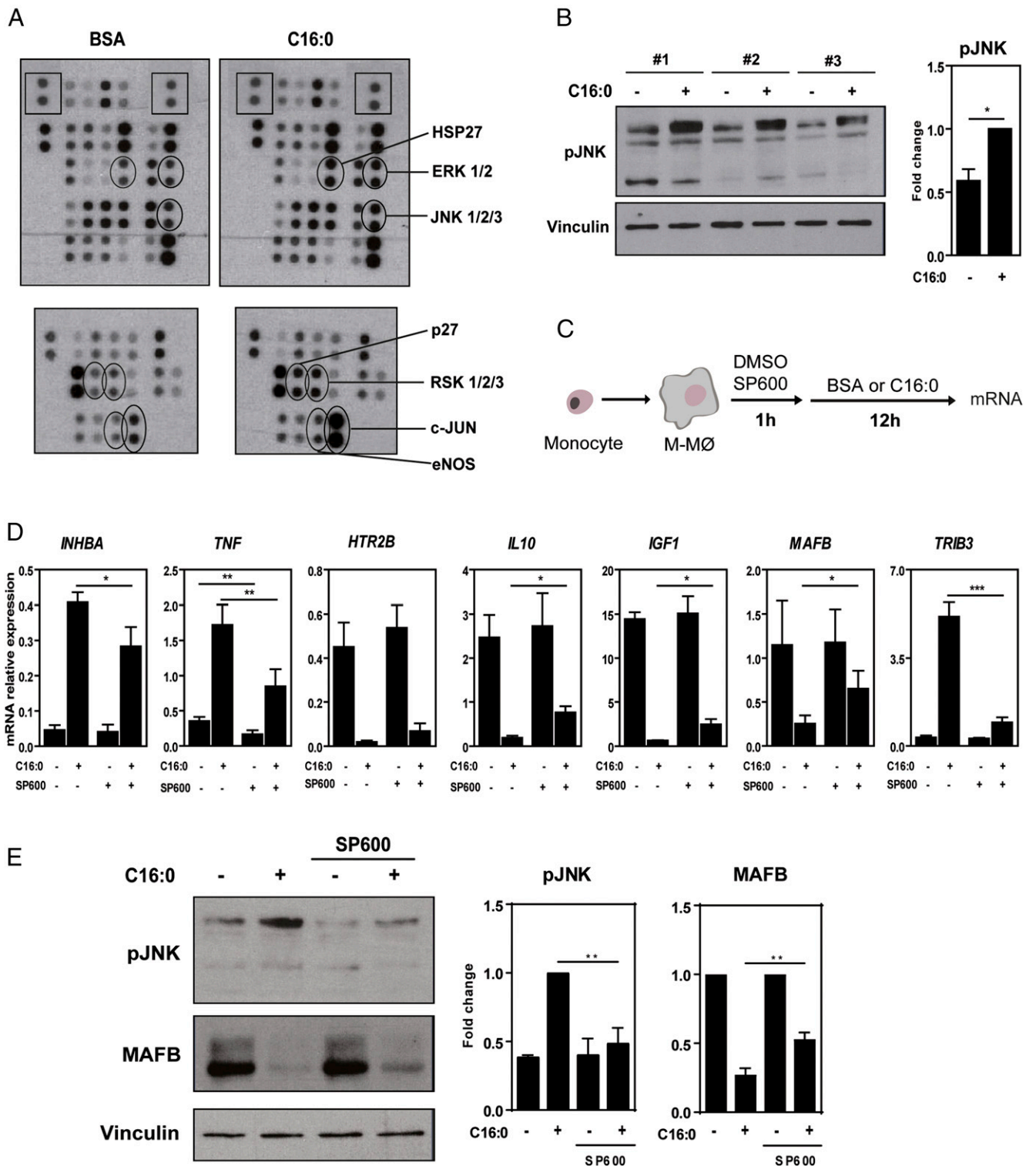
FIGURE 3. Effect of JNK activation on the palmitate-induced transcriptional changes in human macrophages. (**A**) M-MØ were left untreated (BSA) or exposed to 200 μM palmitate (C16:0) for 4 h, and the phosphorylation state of representative signaling molecules was determined using the Proteome Profiler array human phospho-kinase array kit (no. ARY003B; R&D Systems). The kinases specifically mentioned in the text are indicated. The reference spots used for normalization are shown in square boxes at the top of each panel and correspond to a shorter exposure time of the filters. (**B**) M-MØ from three independent donors (nos. 1–3) were left treated with BSA (−) or exposed to 200 μM palmitate (C16:0) for 4 h, and the phosphorylation state of JNK was determined by Western blot using specific Abs. The level of vinculin was determined in parallel as a protein loading control. Right panels show the mean ± SEM of the densitometric analysis of the three experiments. (**C**) Schematic representation of the experimental procedure. (**D**) Relative mRNA expression of the indicated genes in M-MØ exposed to SP600125 (SP600) or DMSO (−) for 1 h and exposed to BSA (−) or 200 μM palmitate (C16:0) for 12 h, as determined by quantitative RT-PCR using *TBP* as a reference. Results are shown as mean ± SEM of five independent experiments. (**E**) JNK activation and MAFB protein levels in M-MØ untreated or exposed to SP600125 (SP600) for 1 h and then exposed to BSA (−) or 200 μM palmitate (C16:0) for 12 h, as determined by determined by Western blot using specific Abs. The level of vinculin was determined in parallel as a protein loading control. The experiment was performed on four independent M-MØ preparations, and one of them is shown. Right panels show the mean ± SEM of the densitometric analysis of the four experiments. *$p < 0.05$, **$p < 0.01$, ***$p < 0.001$.
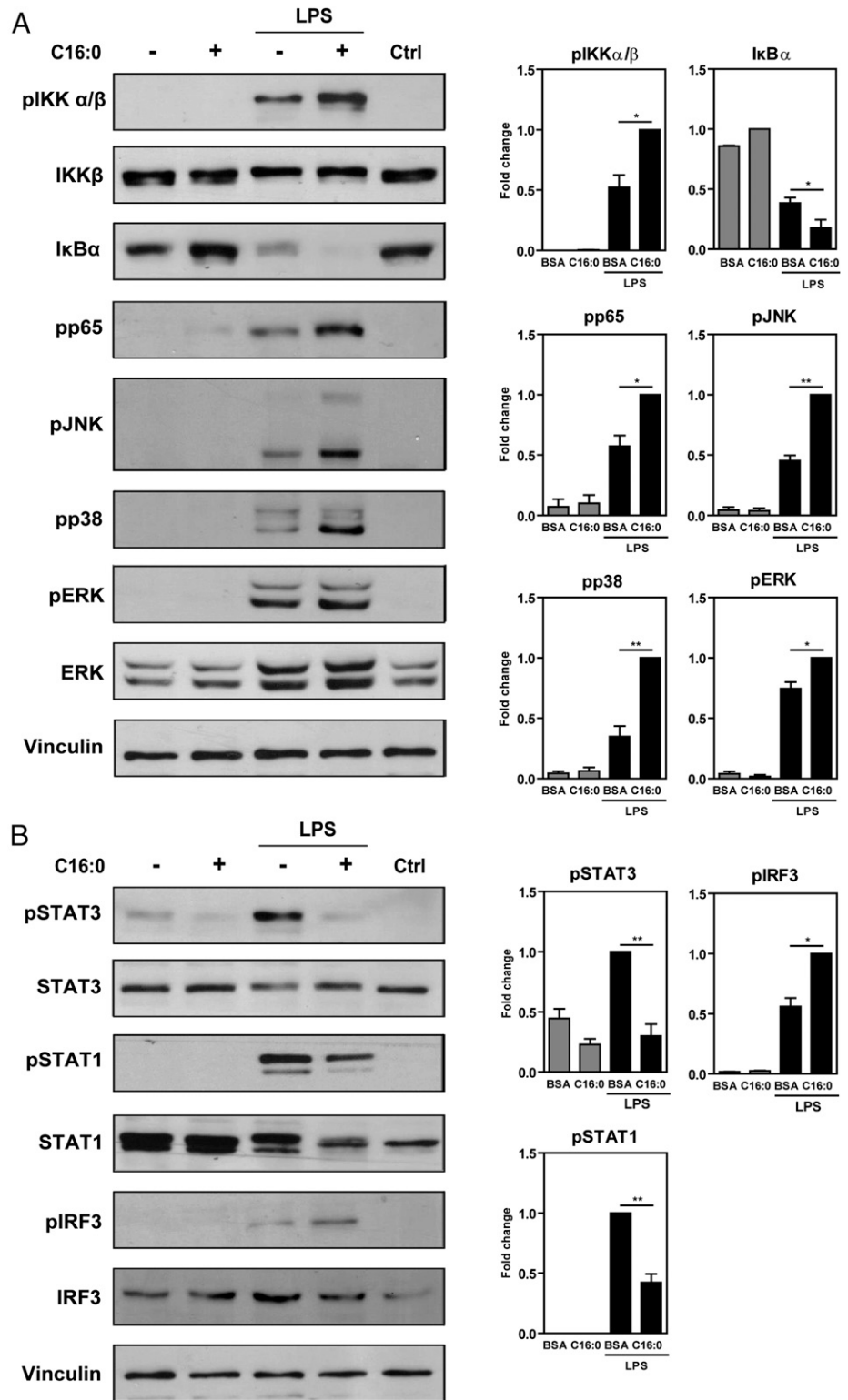
FIGURE 4. Palmitate exposure modulates LPS-initiated intracellular signaling in human macrophages. (**A** and **B**) Determination of the phosphorylation state of (A) IKKα/β, IκBα, NF-κB p65, ERK1/2, JNK, p38 MAPK, STAT3, STAT1, and IRF3 in M-MØ exposed to BSA (−) or palmitate (C16:0) for 24 h and then stimulated with LPS (10 ng/ml) for 15–30 min (A) or 120 min (B). The total levels of IKKα/β, ERK1/2, STAT3, STAT1, and IRF3 were determined in parallel. The levels of vinculin were determined as a protein loading control. The levels of each protein were also determined in untreated cells (Ctrl). In all cases, four independent experiments were performed, and one of them is shown. Right panels show the mean ± SEM of the densitometric analysis of the four experiments. *$p < 0.05$, **$p < 0.01$.

effects on human macrophages. Thus, palmitate and LPS oppositely modulate the expression of genes such as *IDO1*, *MAOA*, *EMR2*, and *LAMB3*. Palmitate and LPS also differ in terms of the intracellular signaling triggered in human macrophages. Palmitate leads to JNK activation at late time points, but causes a very weak NF-κB activation and has no effect on STAT1/STAT3 or IRF3 phosphorylation (Fig. 4). In fact, palmitate pretreatment even reduces the LPS-induced activation of STAT1 and STAT3. This differential signaling ability of palmitate and LPS correlates with their distinct effect on the expression of IFN-regulated genes such

as *IDO1* and strongly suggests that the palmitate-initiated intracellular signaling originates from TLR4 and additional PAMP/damage-associated molecular pattern receptors.

Especially relevant is the fact that palmitate and LPS differentially regulate the expression of *CCL19* and *TRIB3*. Contrary to the effect of LPS, which greatly enhances *CCL19* mRNA (V.D. Cuevas et al., unpublished observations), palmitate significantly downregulates CCL19 at the mRNA and protein level (Fig. 2) and even abrogates the LPS-induced upregulation of CCL19 production (Fig. 6). Together with CCL21, the chemokine CCL19 is a
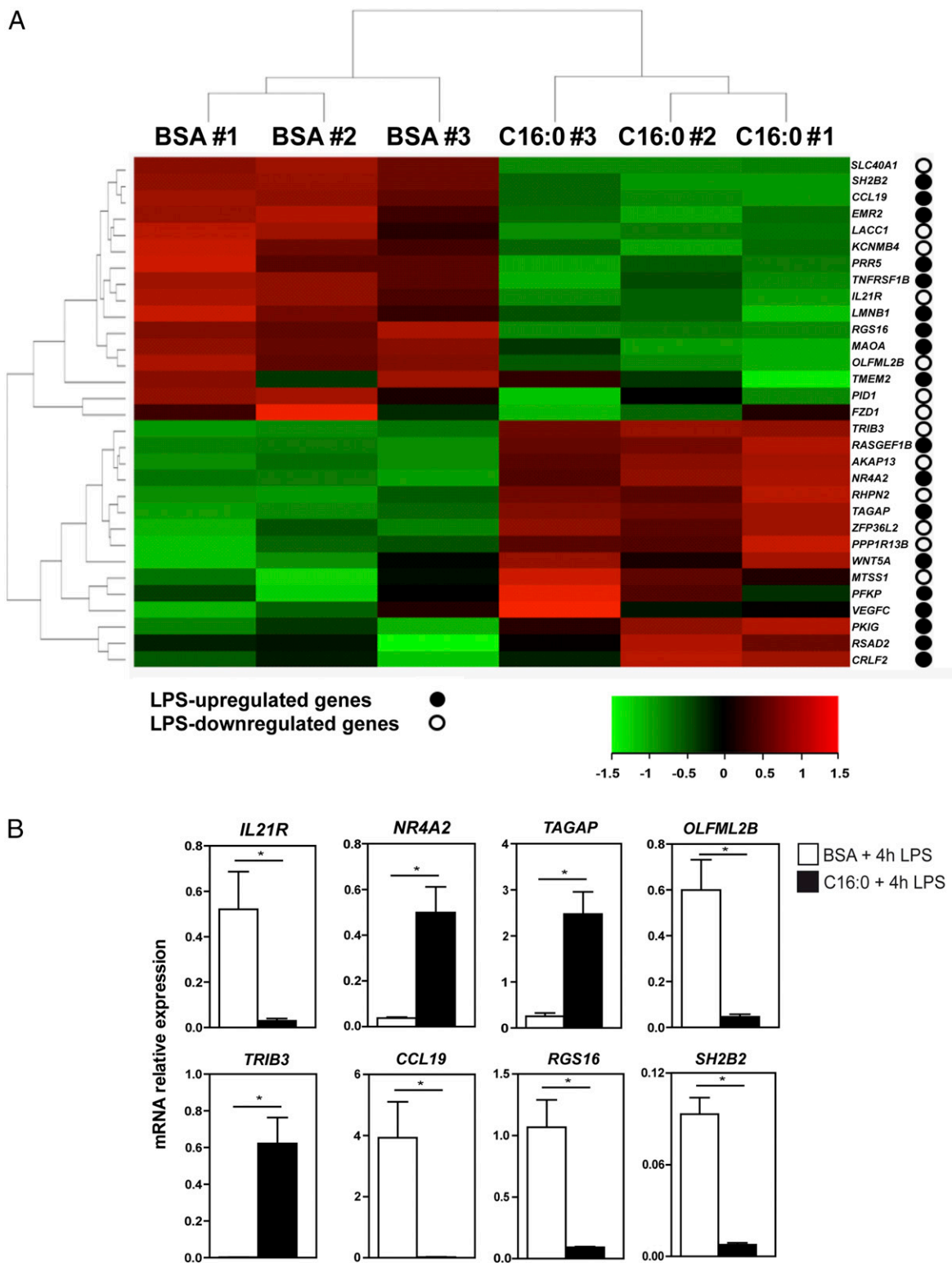
FIGURE 5. Palmitate pretreatment alters the LPS-induced transcriptomic response in human macrophages. (**A**) Heat map representation of the mRNA expression of the LPS-regulated genes whose expression is significantly different ($p < 0.05$) in M-MØ exposed to either BSA or 200 μM palmitate (C16:0) (24 h) before stimulation with LPS (10 ng/ml) for 4 h. The effect of LPS on the expression of the analyzed genes is shown. (**B**) Relative mRNA expression of the indicated genes in M-MØ exposed to either BSA or 200 μM palmitate (C16:0) (24 h) before stimulation with LPS (10 ng/ml) for 4 h, as determined by quantitative RT-PCR using *TBP* as a reference. Shown is the mean ± SEM of three independent experiments. *$p < 0.05$.

ligand of CCR7, whose expression critically determines lymph node homing of T cells and dendritic cells (56). Interestingly, CCL19, but not CCL21, promotes CCR7 phosphorylation, internalization, and desensitization toward CCL21 (56). Therefore, the ability of 200 μM palmitate to ablate the basal and LPS-mediated

CCL19 expression implies that stronger CCR7-dependent responses (dendritic cell homing and maturation, and Ag presentation) (57) must take place in the presence of the palmitate concentrations found in obese individuals. This prediction would be in line with the ability of palmitate to foster the acquisition of
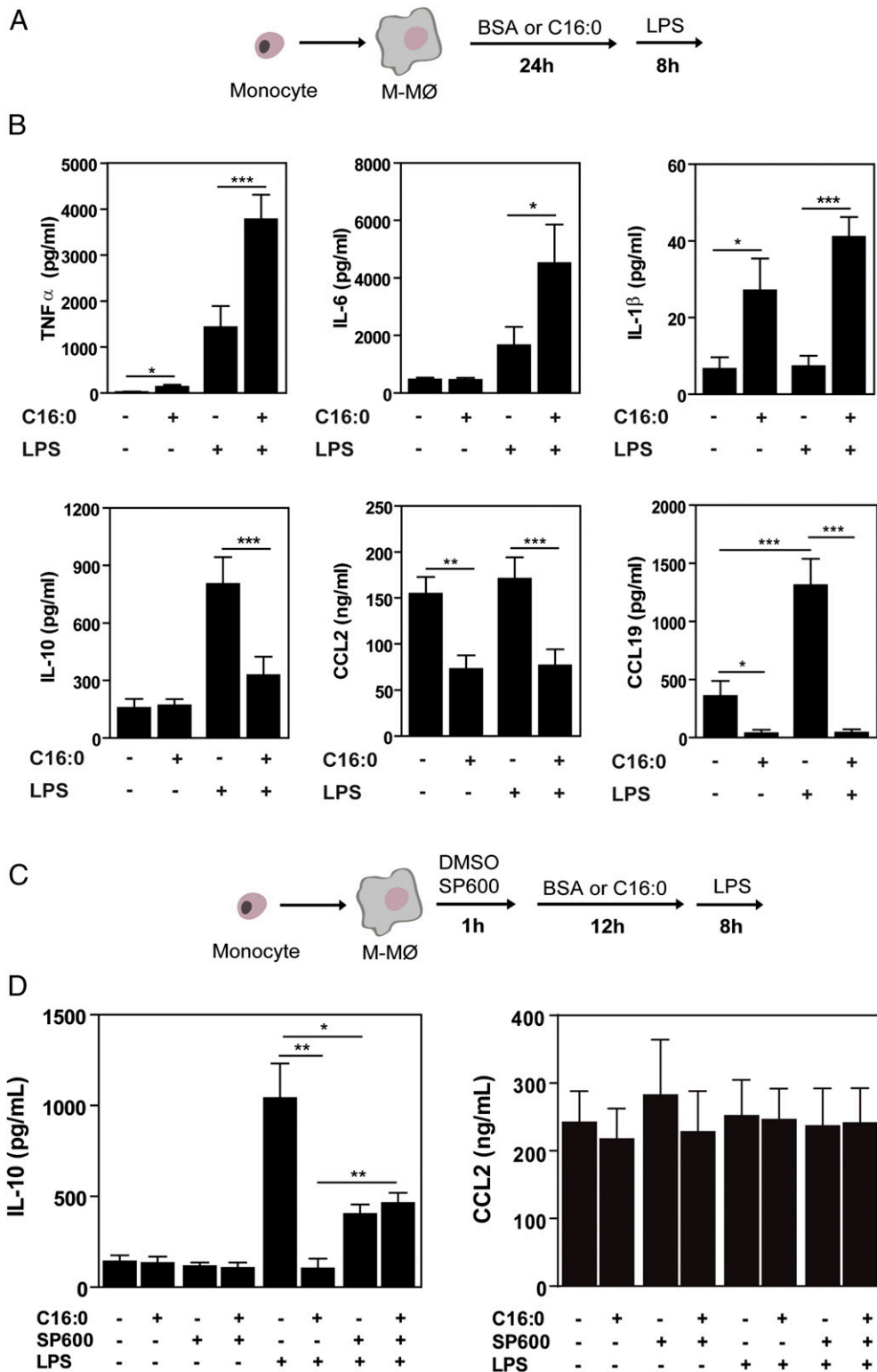
FIGURE 6. Effect of palmitate treatment on the LPS-induced cytokine profile in human macrophages. (**A**) Schematic representation of the experimental procedure. (**B**) Levels of the indicated cytokines in the culture supernatants of macrophages (M-MØ) exposed to 200 μM palmitate (C16:0) or BSA (−) for 24 h before stimulation with 10 ng/ml LPS for 8 h. Shown is the mean ± SEM of eight independent experiments. (**C**) Schematic representation of the experimental procedure. (**D**) Levels of IL-10 and CCL2 in the culture media of macrophages (M-MØ) not treated or treated with SP600125 (SP600), and then exposed to 200 μM palmitate (C16:0) or BSA (−) (24 h) before stimulation with 10 ng/ml LPS (8 h). Shown is the mean ± SEM of four independent experiments. *$p < 0.05$, **$p < 0.01$, ***$p < 0.001$.

the cytokine and transcriptional profile of proinflammatory (and immunogenic) macrophages that we now report.

Regarding the palmitate-mediated upregulation of *TRIB3* gene expression, our results agree with the ability of palmitate to induce

TRIB3 expression in human liver cells (58) and podocytes (59). TRIB3 is a pseudokinase that modulates many signaling cascades associated with endoplasmic reticulum stress, nutrient deficiency, and insulin resistance (60), and it that acts as a negative regulator

of NF-κB–dependent transcription (61). Because TRIB3 negatively regulates CCL2 expression in podocytes (59), it is tempting to speculate that palmitate-induce TRIB3 upregulation might underlie the negative effect that palmitate has on the basal and LPS-induced expression of CCL2 in human macrophages.

Disclosures

The authors have no financial conflicts of interest.

References

1. Gallagher, E. J., and D. LeRoith. 2013. Epidemiology and molecular mechanisms tying obesity, diabetes, and the metabolic syndrome with cancer. *Diabetes Care* 36(Suppl. 2): S233–S239.
2. Hopkins, B. D., M. D. Goncalves, and L. C. Cantley. 2016. Obesity and cancer mechanisms: cancer metabolism. *J. Clin. Oncol.* 34: 4277–4283.
3. Das, U. N. 2001. Is obesity an inflammatory condition? *Nutrition* 17: 953–966.
4. Chawla, A., K. D. Nguyen, and Y. P. Goh. 2011. Macrophage-mediated inflammation in metabolic disease. *Nat. Rev. Immunol.* 11: 738–749.
5. Lumeng, C. N., and A. R. Saltiel. 2011. Inflammatory links between obesity and metabolic disease. *J. Clin. Invest.* 121: 2111–2117.
6. Weisberg, S. P., D. Hunter, R. Huber, J. Lemieux, S. Slaymaker, K. Vaddi, I. Charo, R. L. Leibel, and A. W. Ferrante, Jr. 2006. CCR2 modulates inflammatory and metabolic effects of high-fat feeding. *J. Clin. Invest.* 116: 115–124.
7. Patsouris, D., P. P. Li, D. Thapar, J. Chapman, J. M. Olefsky, and J. G. Neels. 2008. Ablation of CD11c-positive cells normalizes insulin sensitivity in obese insulin resistant animals. *Cell Metab.* 8: 301–309.
8. Arkan, M. C., A. L. Hevener, F. R. Greten, S. Maeda, Z. W. Li, J. M. Long, A. Wynshaw-Boris, G. Poli, J. Olefsky, and M. Karin. 2005. IKK-β links inflammation to obesity-induced insulin resistance. *Nat. Med.* 11: 191–198.
9. Solinas, G., C. Vilcu, J. G. Neels, G. K. Bandyopadhyay, J. L. Luo, W. Naugler, S. Grivennikov, A. Wynshaw-Boris, M. Scadeng, J. M. Olefsky, and M. Karin. 2007. JNK1 in hematopoietically derived cells contributes to diet-induced inflammation and insulin resistance without affecting obesity. *Cell Metab.* 6: 386–397.
10. Shi, H., M. V. Kokoeva, K. Inouye, I. Tzameli, H. Yin, and J. S. Flier. 2006. TLR4 links innate immunity and fatty acid-induced insulin resistance. *J. Clin. Invest.* 116: 3015–3025.
11. Erridge, C., and N. J. Samani. 2009. Saturated fatty acids do not directly stimulate Toll-like receptor signaling. *Arterioscler. Thromb. Vasc. Biol.* 29: 1944–1949.
12. Hosoi, T., S. Yokoyama, S. Matsuo, S. Akira, and K. Ozawa. 2010. Myeloid differentiation factor 88 (MyD88)-deficiency increases risk of diabetes in mice. *PLoS One* 5: e12537.
13. Vijay-Kumar, M., J. D. Aitken, F. A. Carvalho, T. R. Ziegler, A. T. Gewirtz, and V. Ganji. 2011. Loss of function mutation in Toll-like receptor-4 does not offer protection against obesity and insulin resistance induced by a diet high in trans fat in mice. *J. Inflamm.* 8: 2.
14. Hall, E., P. Volkov, T. Dayeh, K. Bacos, T. Rönn, M. D. Nitert, and C. Ling. 2014. Effects of palmitate on genome-wide mRNA expression and DNA methylation patterns in human pancreatic islets. *BMC Med.* 12: 103.
15. Wang, X., Q. Cao, L. Yu, H. Shi, B. Xue, and H. Shi. 2016. Epigenetic regulation of macrophage polarization and inflammation by DNA methylation in obesity. *JCI Insight* 1: e87748.
16. Gordon, S., and P. R. Taylor. 2005. Monocyte and macrophage heterogeneity. *Nat. Rev. Immunol.* 5: 953–964.
17. Escribese, M. M., E. Sierra-Filardi, C. Nieto, R. Samaniego, C. Sánchez-Torres, T. Matsuyama, E. Calderon-Gómez, M. A. Vega, A. Salas, P. Sánchez-Mateos, and A. L. Corbí. 2012. The prolyl hydroxylase PHD3 identifies proinflammatory macrophages and its expression is regulated by activin A. *J. Immunol.* 189: 1946–1954.
18. Sierra-Filardi, E., A. Puig-Kröger, F. J. Blanco, C. Nieto, R. Bragado, M. I. Palomero, C. Bernabéu, M. A. Vega, and A. L. Corbí. 2011. Activin A skews macrophage polarization by promoting a proinflammatory phenotype and inhibiting the acquisition of anti-inflammatory macrophage markers. *Blood* 117: 5092–5101.
19. Soler Palacios, B., L. Estrada-Capetillo, E. Izquierdo, G. Criado, C. Nieto, C. Municio, I. González-Alvaro, P. Sánchez-Mateos, J. L. Pablos, A. L. Corbí, and A. Puig-Kröger. 2015. Macrophages from the synovium of active rheumatoid arthritis exhibit an activin A-dependent pro-inflammatory profile. *J. Pathol.* 235: 515–526.
20. Verreck, F. A., T. de Boer, D. M. Langenberg, M. A. Hoeve, M. Kramer, E. Vaisberg, R. Kastelein, A. Kolk, R. de Waal-Malefyt, and T. H. Ottenhoff. 2004. Human IL-23-producing type 1 macrophages promote but IL-10-producing type 2 macrophages subvert immunity to (myco)bacteria. *Proc. Natl. Acad. Sci. USA* 101: 4560–4565.
21. Lacey, D. C., A. Achuthan, A. J. Fleetwood, H. Dinh, J. Roiniotis, G. M. Scholz, M. W. Chang, S. K. Beckman, A. D. Cook, and J. A. Hamilton. 2012. Defining GM-CSF- and macrophage-CSF-dependent macrophage responses by in vitro models. *J. Immunol.* 188: 5752–5765.
22. Raes, G., R. Van den Bergh, P. De Baetselier, G. H. Ghassabeh, C. Scotton, M. Locati, A. Mantovani, and S. Sozzani. 2005. Arginase-1 and Ym1 are markers for murine, but not human, alternatively activated myeloid cells. *J. Immunol.* 174: 6561, author reply 6561–6562.
23. Izquierdo, E., V. D. Cuevas, S. Fernández-Arroyo, E. Riera-Borrull, E. Orta-Zavalza, J. Joven, E. Rial, A. L. Corbi, and M. M. Escribese. 2015. Reshaping of human macrophage polarization through modulation of glucose catabolic pathways. *J. Immunol.* 195: 2442–2451.
24. Xu, S., Y. Huang, Y. Xie, T. Lan, K. Le, J. Chen, S. Chen, S. Gao, X. Xu, X. Shen, et al. 2010. Evaluation of foam cell formation in cultured macrophages: an improved method with Oil Red O staining and DiI-oxLDL uptake. *Cytotechnology* 62: 473–481.
25. González-Domínguez, É., Á. Domínguez-Soto, C. Nieto, J. L. Flores-Sevilla, M. Pacheco-Blanco, V. Campos-Peña, M. A. Meraz-Ríos, M. A. Vega, A. L. Corbí, and C. Sánchez-Torres. 2016. Atypical activin A and IL-10 production impairs human CD16+ monocyte differentiation into anti-inflammatory macrophages. *J. Immunol.* 196: 1327–1337.
26. Cuevas, V. D., L. Anta, R. Samaniego, E. Orta-Zavalza, J. Vladimir de la Rosa, G. Baujat, Á. Domínguez-Soto, P. Sánchez-Mateos, M. M. Escribese, A. Castrillo, et al. 2017. MAFB determines human macrophage anti-inflammatory polarization: relevance for the pathogenic mechanisms operating in multicentric carpotarsal osteolysis. *J. Immunol.* 198: 2070–2081.
27. Jensen, M. D., M. W. Haymond, R. A. Rizza, P. E. Cryer, and J. M. Miles. 1989. Influence of body fat distribution on free fatty acid metabolism in obesity. *J. Clin. Invest.* 83: 1168–1173.
28. Mittendorfer, B., D. A. Fields, and S. Klein. 2004. Excess body fat in men decreases plasma fatty acid availability and oxidation during endurance exercise. *Am. J. Physiol. Endocrinol. Metab.* 286: E354–E362.
29. Staaf, J., S. J. Ubhayasekera, E. Sargsyan, A. Chowdhury, H. Kristinsson, H. Manell, J. Bergquist, A. Forslund, and P. Bergsten. 2016. Initial hyperinsulinemia and subsequent β-cell dysfunction is associated with elevated palmitate levels. *Pediatr. Res.* 80: 267–274.
30. Ubhayasekera, S. J., J. Staaf, A. Forslund, P. Bergsten, and J. Bergquist. 2013. Free fatty acid determination in plasma by GC-MS after conversion to Weinreb amides. *Anal. Bioanal. Chem.* 405: 1929–1935.
31. Sierra-Filardi, E., C. Nieto, A. Domínguez-Soto, R. Barroso, P. Sánchez-Mateos, A. Puig-Kroger, M. López-Bravo, J. Joven, C. Ardavín, J. L. Rodríguez-Fernández, et al. 2014. CCL2 shapes macrophage polarization by GM-CSF and M-CSF: identification of CCL2/CCR2-dependent gene expression profile. *J. Immunol.* 192: 3858–3867.
32. Kimura, A., T. Naka, T. Nakahama, I. Chinen, K. Masuda, K. Nohara, Y. Fujii-Kuriyama, and T. Kishimoto. 2009. Aryl hydrocarbon receptor in combination with Stat1 regulates LPS-induced inflammatory responses. *J. Exp. Med.* 206: 2027–2035.
33. Ruffell, D., F. Mourkioti, A. Gambardella, P. Kirstetter, R. G. Lopez, N. Rosenthal, and C. Nerlov. 2009. A CREB-C/EBPβ cascade induces M2 macrophage-specific gene expression and promotes muscle injury repair. *Proc. Natl. Acad. Sci. USA* 106: 17475–17480.
34. Huang, S., J. M. Rutkowsky, R. G. Snodgrass, K. D. Ono-Moore, D. A. Schneider, J. W. Newman, S. H. Adams, and D. H. Hwang. 2012. Saturated fatty acids activate TLR-mediated proinflammatory signaling pathways. *J. Lipid Res.* 53: 2002–2013.
35. Pal, D., S. Dasgupta, R. Kundu, S. Maitra, G. Das, S. Mukhopadhyay, S. Ray, S. S. Majumdar, and S. Bhattacharya. 2012. Fetuin-A acts as an endogenous ligand of TLR4 to promote lipid-induced insulin resistance. *Nat. Med.* 18: 1279–1285.
36. Ibrahimi, A., Z. Sfeir, H. Magharaie, E. Z. Amri, P. Grimaldi, and N. A. Abumrad. 1996. Expression of the CD36 homolog (FAT) in fibroblast cells: effects on fatty acid transport. *Proc. Natl. Acad. Sci. USA* 93: 2646–2651.
37. Senn, J. J. 2006. Toll-like receptor-2 is essential for the development of palmitate-induced insulin resistance in myotubes. *J. Biol. Chem.* 281: 26865–26875.
38. Nguyen, M. T., S. Favelyukis, A. K. Nguyen, D. Reichart, P. A. Scott, A. Jenn, R. Liu-Bryan, C. K. Glass, J. G. Neels, and J. M. Olefsky. 2007. A subpopulation of macrophages infiltrates hypertrophic adipose tissue and is activated by free fatty acids via Toll-like receptors 2 and 4 and JNK-dependent pathways. *J. Biol. Chem.* 282: 35279–35292.
39. Xue, J., S. V. Schmidt, J. Sander, A. Draffehn, W. Krebs, I. Quester, D. De Nardo, T. D. Gohel, M. Emde, L. Schmidleithner, et al. 2014. Transcriptome-based network analysis reveals a spectrum model of human macrophage activation. *Immunity* 40: 274–288.
40. Erwig, L. P., D. C. Kluth, G. M. Walsh, and A. J. Rees. 1998. Initial cytokine exposure determines function of macrophages and renders them unresponsive to other cytokines. *J. Immunol.* 161: 1983–1988.
41. Cheng, S. C., J. Quintin, R. A. Cramer, K. M. Shepardson, S. Saeed, V. Kumar, E. J. Giamarellos-Bourboulis, J. H. Martens, N. A. Rao, A. Aghajanirefah, et al. 2014. mTOR- and HIF-1α-mediated aerobic glycolysis as metabolic basis for trained immunity. *Science* 345: 1250684.
42. Netea, M. G., L. A. Joosten, E. Latz, K. H. Mills, G. Natoli, H. G. Stunnenberg, L. A. O'Neill, and R. J. Xavier. 2016. Trained immunity: a program of innate immune memory in health and disease. *Science* 352: aaf1098.
43. Saeed, S., J. Quintin, H. H. Kerstens, N. A. Rao, A. Aghajanirefah, F. Matarese, S. C. Cheng, J. Ratter, K. Berentsen, M. A. van der Ent, et al. 2014. Epigenetic programming of monocyte-to-macrophage differentiation and trained innate immunity. *Science* 345: 1251086.
44. Han, M. S., D. Y. Jung, C. Morel, S. A. Lakhani, J. K. Kim, R. A. Flavell, and R. J. Davis. 2013. JNK expression by macrophages promotes obesity-induced insulin resistance and inflammation. *Science* 339: 218–222.
45. Ray, I., S. K. Mahata, and R. K. De. 2016. Obesity: an immunometabolic perspective. *Front. Endocrinol. (Lausanne)* 7: 157.
46. Kratz, M., B. R. Coats, K. B. Hisert, D. Hagman, V. Mutskov, E. Peris, K. Q. Schoenfelt, J. N. Kuzma, I. Larson, P. S. Billing, et al. 2014. Metabolic

dysfunction drives a mechanistically distinct proinflammatory phenotype in adipose tissue macrophages. *Cell Metab.* 20: 614–625.

47. Johnson, A. R., J. J. Milner, and L. Makowski. 2012. The inflammation highway: metabolism accelerates inflammatory traffic in obesity. *Immunol. Rev.* 249: 218–238.

48. Cani, P. D., J. Amar, M. A. Iglesias, M. Poggi, C. Knauf, D. Bastelica, A. M. Neyrinck, F. Fava, K. M. Tuohy, C. Chabo, et al. 2007. Metabolic endotoxemia initiates obesity and insulin resistance. *Diabetes* 56: 1761–1772.

49. Blair, A., N. J. Goulden, N. A. Libri, A. Oakhill, and D. H. Pamphilon. 2005. Immunotherapeutic strategies in acute lymphoblastic leukaemia relapsing after stem cell transplantation. *Blood Rev.* 19: 289–300.

50. Odegaard, J. I., and A. Chawla. 2011. Alternative macrophage activation and metabolism. *Annu. Rev. Pathol.* 6: 275–297.

51. Ortiz, S., P. Zapater, J. L. Estrada, P. Enriquez, M. Rey, A. Abad, J. Such, F. Lluis, and R. Francés. 2014. Bacterial DNA translocation holds increased insulin resistance and systemic inflammatory levels in morbid obese patients. *J. Clin. Endocrinol. Metab.* 99: 2575–2583.

52. Tanahashi, H., K. Kito, T. Ito, and K. Yoshioka. 2010. MafB protein stability is regulated by the JNK and ubiquitin-proteasome pathways. *Arch. Biochem. Biophys.* 494: 94–100.

53. Herath, N. I., N. Rocques, A. Garancher, A. Eychène, and C. Pouponnot. 2014. GSK3-mediated MAF phosphorylation in multiple myeloma as a potential therapeutic target. *Blood Cancer J.* 4: e175.

54. Choi, S. E., Y. Kang, H. J. Jang, H. C. Shin, H. E. Kim, H. S. Kim, H. J. Kim, D. J. Kim, and K. W. Lee. 2007. Involvement of glycogen synthase kinase-3β in palmitate-induced human umbilical vein endothelial cell apoptosis. *J. Vasc. Res.* 44: 365–374.

55. Phiel, C. J., and P. S. Klein. 2001. Molecular targets of lithium action. *Annu. Rev. Pharmacol. Toxicol.* 41: 789–813.

56. Förster, R., A. C. Davalos-Misslitz, and A. Rot. 2008. CCR7 and its ligands: balancing immunity and tolerance. *Nat. Rev. Immunol.* 8: 362–371.

57. Sánchez-Sánchez, N., L. Riol-Blanco, and J. L. Rodríguez-Fernández. 2006. The multiple personalities of the chemokine receptor CCR7 in dendritic cells. *J. Immunol.* 176: 5153–5159.

58. Yan, W., Y. Wang, Y. Xiao, J. Wen, J. Wu, L. Du, and W. Cai. 2014. Palmitate induces TRB3 expression and promotes apoptosis in human liver cells. *Cell. Physiol. Biochem.* 33: 823–834.

59. Morse, E., J. Schroth, Y. H. You, D. P. Pizzo, S. Okada, S. Ramachandrarao, V. Vallon, K. Sharma, and R. Cunard. 2010. TRB3 is stimulated in diabetic kidneys, regulated by the ER stress marker CHOP, and is a suppressor of podocyte MCP-1. *Am. J. Physiol. Renal Physiol.* 299: F965–F972.

60. Mondal, D., A. Mathur, and P. K. Chandra. 2016. Tripping on TRIB3 at the junction of health, metabolic dysfunction and cancer. *Biochimie* 124: 34–52.

61. Wu, M., L. G. Xu, Z. Zhai, and H. B. Shu. 2003. SINK is a p65-interacting negative regulator of NF-kappaB-dependent transcription. *J. Biol. Chem.* 278: 27072–27079.